Functional Expression of cDNA Encoding the Ca^{2+} Release Channel (Ryanodine Receptor) of Rabbit Skeletal Muscle Sarcoplasmic Reticulum in COS-1 Cells†

S. R. Wayne Chen,‡ Donna M. Vaughan,§ Judith A. Airey,‖ Roberto Coronado,*,§ and David H. MacLennan*,‡

Banting and Best Department of Medical Research, University of Toronto, C. H. Best Institute, Toronto, Ontario M5G 1L6, Canada, Department of Physiology, University of Wisconsin School of Medicine, Madison, Wisconsin 53706, and Department of Pharmacology and Cell and Molecular Biology Program, University of Nevada, Reno, Nevada 89557

Received June 8, 1992; Revised Manuscript Received November 30, 1992

ABSTRACT: A full-length cDNA encoding the ryanodine receptor of rabbit skeletal muscle sarcoplasmic reticulum was transiently expressed in COS-1 cells. Immunoblotting studies showed that the expressed ryanodine receptor and the native ryanodine receptor of rabbit skeletal muscle were indistinguishable in molecular size and immunoreactivity. Scatchard analysis of [^{3}H]ryanodine binding to transfected COS-1 cell microsomes resulted in a B_{max} of 0.22 pmol/mg of protein and a K_d of 16.2 nM. Expressed ryanodine receptors were solubilized in CHAPS and were shown to cosediment with native ryanodine receptors in a sucrose density gradient. Thus, the expressed receptor, like the native receptor, is assembled as a large oligomeric complex. Single-channel recordings in planar lipid bilayers were used to investigate the functional properties of the sucrose gradient-purified complex. The expressed ryanodine receptor formed a large conductance channel activated by ATP and Ca^{2+} and inhibited by Mg^{2+} and ruthenium red. Ryanodine reduced the conductance and increased the mean open time in a manner consistent with that of native channels. These results demonstrated that functional binding sites for the physiological ligands (Ca^{2+}, Mg^{2+}, and ATP) and pharmacological ligands (ruthenium red and ryanodine) controlling gating of the Ca^{2+} release channel are encoded in the ryanodine receptor cDNA and are faithfully expressed in COS-1 cells. Ryanodine receptors expressed in COS-1 cells displayed several conductance states ≥1 nS not present in native channels. Such anomalous conductance states of the expressed channel might be referable to lack of muscle-specific posttranslational processing or to the need for components not present in COS-1 cells, which may be required to stabilize the channel structure.

Muscle contraction is triggered by a rapid release of Ca^{2+} from the sarcoplasmic reticulum in response to electrical stimulation of the muscle cell surface [reviewed by Endo (1985)]. The channel responsible for the increase in sarcoplasmic reticulum Ca^{2+} permeability appears to be the ryanodine receptor which is located in the terminal cisternae (Inui et al., 1987; Imagawa et al., 1987; Lai et al., 1988; Anderson et al., 1989; Rardon et al., 1989). The ryanodine receptor also forms part of the "foot" structure that bridges the gap between the terminal cisternae membrane and the transverse tubular membrane (Block et al., 1988; Saito et al., 1988; Wagenknecht et al., 1989). The mechanism by which ryanodine receptors open in response to depolarization during excitation–contraction coupling is currently unknown. Hypotheses range from protein–protein coupling between voltage sensors and ryanodine receptors to the activation of ryanodine receptors by Ca^{2+} entry into the cell or by a second messenger produced during depolarization [reviewed by Rios and Pizarro (1991)]. Clues about the function of this channel have been provided by single-channel recordings in planar bilayers. The purified complex forms a large conductance channel, permeable to monovalent and divalent cations, which is activated by micromolar Ca^{2+}, and to a lesser extent by millimolar ATP,[1] and is strongly inhibited by millimolar Mg^{2+} and micromolar ruthenium red (Lai et al., 1988; Hymel et al., 1988; Smith et al., 1988). Hence, the channel could function in situ as a Ca^{2+}-activated channel with an activity modulated by the cytosolic ligands Mg^{2+} and ATP. These studies have led to the suggestion that ligand binding sites for channel activation and inhibition may be located within the primary structure of the protein although, until the present work, this had not been established.

Cloning and sequencing of cDNA encoding the ryanodine receptor have provided important information regarding its primary and predicted secondary structure (Takeshima et al., 1989; Zorzato et al., 1990). The rabbit skeletal muscle ryanodine receptor cDNA encodes a protein of 5037 amino acids with a mass of 564 000 daltons, made without an NH_2-terminal signal sequence. Sequence analysis has revealed that approximately one-fifth of the COOH terminus of the molecule is likely to form the transmembrane region of the Ca^{2+} conducting pore. The remaining portion of the molecule is hydrophilic and apparently constitutes the cytoplasmic "foot" domain. The rabbit skeletal muscle ryanodine receptor cDNA has been expressed in Chinese hamster ovary (CHO) cells (Takeshima et al., 1989; Penner et al., 1989). Whole cell

† This research was supported by Grant MT-3399 to D.H.M. from the Medical Research Council of Canada and by grants to R.C. from the National Institutes of Health (GM36852), the American Heart Association, and the Muscular Dystrophy Association. S.R.W.C. is a postdoctoral fellow of the Medical Research Council of Canada; D.M.V. is a predoctoral fellow of the Wisconsin affiliate of the American Heart Association.

* To whom correspondence should be addressed.
‡ University of Toronto.
§ University of Wisconsin School of Medicine.
‖ University of Nevada.

[1] Abbreviations: ATP, adenosine 5′-triphosphate; BCIP, 5-bromo-4-chloro-3-indolyl phosphate; NBT, nitroblue tetrazolium; DAB, 3,3′-diaminobenzidine tetrahydrochloride dihydrate; DTT, dithiothreitol; EDTA, ethylenediaminetetraacetic acid; PMSF, phenylmethanesulfonyl fluoride; SDS, sodium dodecyl sulfate; HEPES, 4-(2-hydroxyethyl)-1-piperazineethanesulfonic acid; CHAPS, 3-[(3-cholamidopropyl)dimethylammonio]-1-propanesulfonic acid; PBS, phosphate-buffered saline; TBS, Tris-buffered saline; ELISA, enzyme-linked immunoabsorbent assay.

0006-2960/93/0432-3743$04.00/0

measurements showed that caffeine or ryanodine was capable of inducing Ca^{2+} release from intracellular organelles of the transformed CHO cells, but not from nontransfected control CHO cells (Penner et al., 1989). However, in those studies, the channel was not isolated and characterized directly so that its kinetics and responses to modulators such as Ca^{2+}, ATP, Mg^{2+}, or ruthenium red were not analyzed.

The issue of whether the ryanodine receptor gene encodes a Ca^{2+} channel gated by cytosolic ligands was recently contested by Zaidi et al. (1989). In their study, a 106-kDa protein was isolated from skeletal muscle sarcoplasmic reticulum and was shown to form a channel with characteristics similar to the native ryanodine receptor, such as activation by Ca^{2+} and ATP and inhibition by Mg^{2+} and ruthenium red. Since the 106-kDa protein could be detected throughout a linear sucrose density gradient, in which the ryanodine receptor migrates toward the bottom, it was argued that preparations of purified ryanodine receptors contained the 106-kDa protein and that the latter, rather than the former, formed the Ca^{2+} release channel. To establish whether a single cDNA encoding the 564-kDa ryanodine receptor subunit could form pharmcologically correct Ca^{2+} release channels, the cDNA encoding the rabbit skeletal muscle ryanodine receptor was expressed in COS-1 cells and was characterized by immunoblotting, radioligand binding, and sedimentation. The channel kinetics and ligand-gating properties of the expressed protein were studied by single-channel recordings in planar lipid bilayers. Parts of this work were presented in abstract form (Chen et al., 1992; Vaughan et al., 1992).

EXPERIMENTAL PROCEDURES

Materials. Ryanodine was obtained from AgriSystems International (Wind Gap, PA). [^{3}H]Ryanodine (54.7 Ci/mmol) was purchased from Dupont, New England Nuclear. Soybean phosphatidylcholine, brain phosphatidylethanolamine, and brain phosphatidylserine were obtained from Avanti Polar Lipids. Restriction endonucleases and DNA-modifying enzymes were purchased from Boehringer Mannhein, Bethesda Research Laboratories, and Pharmacia LKB Biotechnology Inc. Monoclonal antibody 34C was generated as described by Airey et al. (1990). A52 is a monoclonal antibody against the fast-twitch muscle Ca^{2+}-ATPase (Maruyama & MacLennan, 1988). Horseradish peroxidase-conjugated goat anti-mouse IgG was obtained from Jackson Immuno Research Laboratories. Alkaline phosphatase-conjugated anti-mouse IgG was obtained from Promega Biotech. CHAPS, NBT, BCIP, and DAB were purchased from Sigma. Nitrocellulose membranes were from Schleicher & Schuell.

Sarcoplasmic Reticulum Preparation. Heavy sarcoplasmic reticulum was isolated from rabbit fast-twitch skeletal muscle as described by Campbell and MacLennan (1981). The vesicles were suspended in 0.25 M sucrose, 10 mM Tris-HCl, pH 8.0, and 1 mM histidine and stored at −70 °C.

Construct for Expression. All recombinant DNA manipulations were carried out by standard procedures (Sambrook et al., 1989). The cloning and sequencing of cDNA encoding the rabbit skeletal muscle ryanodine receptor were described previously (Zorzato et al., 1990). Four overlapping clones were isolated and subcloned into the *Eco*RI site in the Bluescript vector for pBS-SRR2, pBS-SRR3, and pBS-SRR4 and into the *Bam*HI site for pBS-SRR1 and used for constructing the full-length expression plasmid pSRRI as follows (Figure 1). The *Bam*HI (4893)/*Xho*I (6469) fragment from pBS-SRR2 was ligated with the *Bam*HI (4893)/*Xho*I (vector) fragment from pBS-SRR3 [in which the *Bam*HI (vector) was removed] to yield pBS-SRR5. The *Aat*II (3334)/*Xho*I (6469) fragment from pBS-SRR5 was ligated with the *Aat*II (3334)/*Xho*I (vector) fragment from pBS-SRR4 to form pBS-SRR6. The *Stu*I (8820)/*Eco*RI (11623) fragment from pBS-SRR1 was ligated with the *Stu*I (8820)/*Eco*RI (vector) fragment from pBS-SRR2a which was formed by removing the *Bam*HI (vector)/*Bam*HI (4893) fragment containing the *Eco*RI (vector) from pBS-SRR2 to yield pBS-SRR7. The *Xho*I (6469)/*Xho*I (vector) fragment from pBS-SRR7 was ligated with the *Xho*I (6469)/*Xho*I (vector) fragment from pBS-SRR6 to yield pBS-SRR8. The *Nde*I (11159)/*Hin*dIII (vector) fragment from pBS-SRR1 was ligated with the *Nde*I (11159)/*Hin*dIII (vector) fragment from pBS-SRR8 to yield pBS-SRR9. The *Hin*dIII site (vector) in pBS-SRR9 was changed to *Xba*I by blunt-ending with Klenow (Boehringer Mannhein) and ligating the blunt-ended fragment with an *Xba*I linker to yield pBS-SRR10. Finally, the 15.5-kb *Xba*I fragment carrying the entire protein-coding region from pBS-SRR10 was subcloned into the *Xba*I site of the expression vector pMT2(*Cla*I,*Xba*I), a gift from Dr. Randal Kaufman, Genetics Institute, Boston, to yield pSRRI. The *Eco*RI fragment carrying the full-length cDNA encoding the fast-twitch muscle Ca^{2+}-ATPase was removed from p91023(B) (Maruyama & MacLennan, 1988) and subcloned into the *Eco*RI site of the expression vector pMT2-(*Cla*I,*Xba*I).

Cell Culture and DNA Transfection. COS-1 cells were maintained in Dulbecco's modified Eagle's medium (DMEM) as described earlier (Maruyama & MacLennan, 1988). DNA transfection was carried out using the DEAE-dextran method (Gorman, 1985) with some modifications. Cells were washed 3 times with TBS (10 mM Tris-HCl, pH 7.5, and 150 mM NaCl) and transfected with 4.5 mL of TBS solution containing 8 μg of cesium chloride gradient purified DNA and 1 mg/mL DEAE-dextran. Cells were then incubated with 8 mL of chloroquine (1 μg/mL) in DMEM for 3.5 h at 37 °C, washed with TBS, and grown in DMEM for 40–48 h. Control cells were treated in the same way with no DNA or with plasmids containing oppositely-oriented cDNA.

Membrane Preparations from COS-1 Cells. Membrane preparations were carried out as described by Maruyama and MacLennan (1988) with some modifications. All of the following steps were carried out either on ice or in a 4 °C cold room. Cells grown on 10-cm tissue culture dishes were washed twice with 3 mL of PBS containing 0.5 mM PMSF, 2 mM iodoacetamide, 1 mM benzamidine, 1 μg/mL leupeptin, 1 μg/mL pepstatin A, 1 μg/mL aprotinin, 0.1 mg/mL bacitracin, and 5 mM EDTA and harvested in the same solution by scraping. Cells were collected by centrifugation at 10 000 rpm for 10 min in a Sorvall SS-34 rotor. Cell pellets were washed with the above solution without EDTA, pelleted again, and suspended in a solution containing 25 mM Tris–HEPES, pH 7.4, 0.5 mM $MgCl_2$, and a protease inhibitor mix (0.5 mM PMSF, 1 mM benzamidine, 2 μg/mL Leupeptin, 1 μg/mL pepstatin A, 1 μg/mL aprotinin, 1 mg/mL bacitracin, and 5 mM DTT). Cells were homogenized in a Teflon–glass Dounce homogenizer for 50 strokes with pestle A. An equal volume of a solution containing 25 mM Tris–HEPES, pH 7.4, 0.5 M sucrose, 0.3 M KCl, 40 μM $CaCl_2$, and the protease inhibitor mix was added to the homogenates and homogenized for 25 strokes. The suspension was centrifuged at 6000 rpm for 20 min in a Sorvall SS-34 rotor at 4 °C. The supernatant was centrifuged at 35 000 rpm in a Beckman Ti60 rotor for 90 min. The pellets were suspended in a buffer containing 25 mM Tris–HEPES, pH 7.4, 0.3 M sucrose, 0.15 M KCl, 20 μM $CaCl_2$, and protease inhibitor mix and stored at −70 °C.

Immunocytochemical Staining. A glass slide was placed in a 10-cm tissue culture dish. Cell culture and DNA transfection were then carried out as described above. The growth medium was discarded 40–48 h after transfection. The glass slide was washed 3 times with PBS, fixed with 4% formaldehyde in PBS for 15 min, and washed with PBS and PBS containing 0.1% saponin for 5 min each time. The slide was blocked with buffer A (2% skim milk powder/0.1% saponin in PBS) for 30 min before being washed and incubated with monoclonal antibody 34C in buffer A for 1–2 h. The slide was washed with buffer A and incubated with horseradish peroxidase-conjugated anti-mouse IgG in buffer A for 30–60 min. The sample was then washed, and the bound antibodies were detected by their reaction in buffer A with 0.2 mg/mL DAB, 0.03% H_2O_2, and 0.01% cobalt chloride.

[^{3}H]Ryanodine Binding Assay. Membrane preparations (0.5–1 mg/mL) were incubated with various concentrations (1–60 nM) of [^{3}H]ryanodine for 1 h at 37 °C in 0.2 mL of a solution containing 25 mM Na-Pipes, pH 7.4, 1.5 M KCl, 0.2 M sucrose, 10 mM ATP, 0.8 mM $CaCl_2$, and protease inhibitor mix. The amount of [^{3}H]ryanodine bound was determined by filtration through Whatman GF/B membranes presoaked with 1% poly(ethylenimine). The filters were washed 4 times with 4 mL of an ice-cold solution containing 25 mM Tris-HCl, pH 7.4, 0.5 M KCl, and 250 μM $CaCl_2$. The radioactivities associated with the filters were determined by liquid scintillation counting. Nonspecific binding was determined by measuring [^{3}H]ryanodine binding in the presence of 30 μM unlabeled ryanodine. All binding assays were carried out in duplicate.

Solubilization and Sucrose Density Gradient Centrifugation. Membrane preparations (2.5 mg/mL) were solubilized in a solution containing 50 mM Tris–HEPES, pH 7.4, 0.5% CHAPS, 1 M NaCl, 0.25 mM PMSF, 1 mM iodoacetamide, 1 mM benzamidine, 1 μg/mL leupeptin, 1 μg/mL pepstatin A, and 1 μg/mL aprotinin for 90 min at 0 °C. The suspension was spun at 35 000 rpm in a Beckman Ti60 rotor for 1 h at 4 °C, and 2 mL of the supernatant was layered on top of a 10-mL (10–30% w/v) linear sucrose gradient containing 50 mM Tris–HEPES, pH 7.4, 0.3 M NaCl, 0.1 mM $CaCl_2$, 0.25 mM PMSF, 1 μg/mL leupeptin, 2 mM DTT, 0.3% CHAPS, and 0.15% L-phosphatidylcholine. The tubes were centrifuged at 30 000 rpm in a Beckman SW-40 rotor for 17 h at 4 °C. Fractions of 0.5 mL each were collected and monitored for protein content and immunoreactivity by immunoblotting and enzyme-linked immunoabsorbent assay. The peak fractions of immunoreactivity were concentrated up to 30-fold in volume in Centricon-100 microconcentrators (Amicon) and stored at −70 °C. Aliquots of frozen samples were used for single-channel measurements.

Enzyme-Linked Immunoabsorbent Assay. Aliquots of 10–50 μL of the sucrose density gradient fractions were added to microtiter wells containing 150 μL of 50 mM sodium carbonate buffer, pH 9.6. The microtiter plate was incubated at 4 °C for 18 h and then blocked with 5% skim milk powder in 50 mM sodium carbonate buffer, pH 9.6, for 1 h at room temperature. The plate was washed 3 times with PBS solution containing 5% milk powder and 0.1% Tween-20, incubated with monoclonal antibody 34C in the same buffer for 2–4 h, washed again, and allowed to react with alkaline phosphatase-conjugated anti-mouse IgG for 1 h. The samples were again washed, and bound antibodies were quantitated by the alkaline phosphatase reaction in diethanolamine buffer containing 10% diethanolamine, pH 9.8, 5 mM $MgCl_2$, and one phosphatase substrate tablet (Sigma) per 5 mL of diethanolamine buffer.

Planar Lipid Bilayer Methods. Planar bilayers were cast from brain phosphatidylethanolamine and brain phosphatidylserine (Avanti Polar Lipids, Birmingham, AL) as described by Coronado et al. (1992). Lipids were mixed at a weight ratio of 1:1 and dissolved in decane (Aldrich, Milwaukee, WI) at a concentration of 20 mg of lipid/mL. Bilayers were formed on a 0.3-mm-diameter hole in a Lexan polycarbonate partition. A solution composed of 380 mM CsCl in 10 mM HEPES, adjusted to pH 7.3 with Tris, was added to both cis (1 mL) and trans (3 mL) compartments. Channels were incorporated into preformed planar bilayers by a detergent dilution procedure similar to that used for the recording of purified native receptors (Smith et al., 1988). A 10–30-μL aliquot of concentrated sucrose density gradient fractions (3–5 mg/mL) was added to the 1-mL cis solution while stirring with a magnetic stirrer. Channel incorporation was induced by repetitive breakage and re-formation of bilayers. The same cis solution was used for several separate recordings for up to 2 h, depending on the protocol. The cis side was connected to the head-stage input of a List L/M EPC 7 amplifier (List Electronic, DA-Eberstadt, FRG) by a Ag/AgCl electrode and an agar/KCl bridge. The trans solution was held at ground potential using the same electrode arrangement. Recordings were filtered through a low-pass Bessel filter (Frequency Devices, Haverhill, MA) at 1 kHz and digitized at 5–10 kHz. Data were acquired on VHS videotape, digitized upon playback, and stored on high-capacity Bernoulli disks using Axotape 1.2.01 software (Axon Instruments, Inc.). Data analysis was done on a PC/AT computer using pClamp 5.5 software (Axon Instruments, Inc.). The total recording time stored on tape was greater than 20 h, reflecting a minimum of 44 separate bilayers.

Polyacrylamide Gel Electrophoresis and Immunoblotting. Membrane proteins (5–50 μg) were denatured in Laemmli sample buffer at 100 °C for 2 min and separated in a 5% SDS–polyacrylamide minigel (Laemmli, 1970). A constant voltage of 50 V was applied for the first 90 min, and then 150 V was applied. The resolved proteins were transferred to nitrocellulose membranes at 50 V for 4 h at 4 °C according to Towbin et al. (1979). The membranes were blocked for 1 h with a solution of 10 mM Tris-HCl, pH 8.0, 150 mM NaCl, 0.1% Tween-20, and 5% skim milk powder, incubated overnight with monoclonal antibody 34C in the same solution, and washed 3 times with the same solution. Bound antibodies were then visualized by the alkaline phosphatase reaction using alkaline phosphatase-conjugated anti-mouse IgG with NBT and BCIP as substrates.

Protein Assay. Proteins were measured according to Lowry et al. (1951) using bovine serum albumin as a standard.

RESULTS

Transient Expression of Ryanodine Receptor cDNA. The COS-1 cell expression system has been used successfully to express and characterize several sarcoplasmic reticulum proteins (Maruyama & MacLennan, 1988; Leberer et al., 1989; Fujii et al., 1989). Because COS-1 cells produce the large T antigen, expression plasmids containing the SV40 origin of replication are replicated in high copy number in transfected cells. The expression plasmid pSRRI, carrying the entire protein-coding sequence, linked to the adenovirus major late promoter and SV40 origin of replication, was constructed (Figure 1) and used to transfect COS-1 cells. Transient expression of the ryanodine receptor was detected by immunoblotting with mAb 34C raised against the avian skeletal muscle ryanodine receptor (Figure 2) (Airey et al., 1990). A major high molecular weight band was recognized

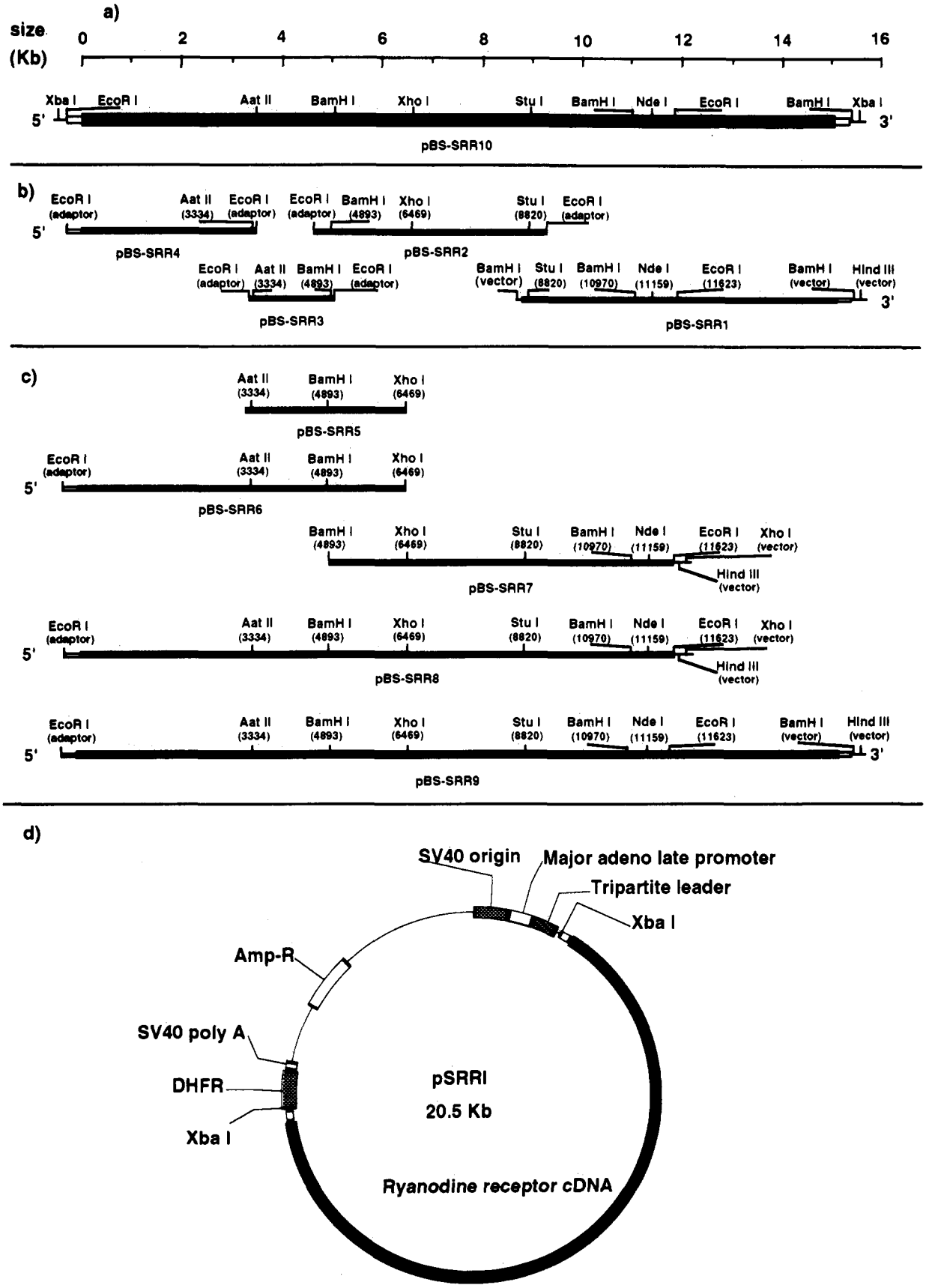

FIGURE 1: Construction of the expression plasmid pSRRI from the rabbit skeletal muscle ryanodine receptor cDNA and the vector pMT2(*ClaI*,*XbaI*) (Kaufman et al., 1989). Restriction endonuclease sites used for construction are shown. The protein coding region is indicated by a closed box, the 5′- and 3′-noncoding regions by open boxes, and vector DNA by a solid line. (a) pBS-SRR10, the full-length cDNA insert for pSRRI. (b) Original cDNA clones used in the construction of pBS-SRR10 and pSRRI. (c) Plasmids generated during the construction. (d) Schematic representation of pSRRI. The closed box represents ryanodine receptor cDNA.

by mAb 34C in membrane preparations from COS-1 cells transfected with pSRRI, but was not detected in membrane preparations from COS-1 cells transfected either with no DNA or with a plasmid with oppositely-oriented cDNA. The major

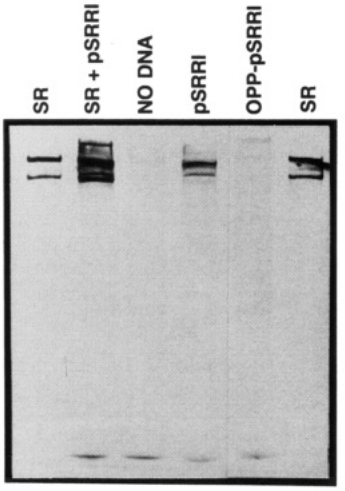

FIGURE 2: Expression of the skeletal muscle ryanodine receptor in COS-1 cells. DNA transfection and membrane preparation were carried out as described under Experimental Procedures. Membrane proteins (50 μg) from COS-1 cells transfected with pSRRI, no DNA, or plasmid with oppositely-oriented cDNA (OPP-pSRRI) or from the sarcoplasmic reticulum (SR) (5 μg) were solubilized in Laemmli SDS sample buffer and separated by 5% SDS–PAGE. Ryanodine receptor proteins were detected by immunoblotting using monoclonal antibody 34C and secondary alkaline phosphatase-conjugated anti-mouse IgG. The upper band in the SR lanes corresponds to the full-length ryanodine receptor of 564 000 daltons; the lower band is a degradation product. Staining of small fragments also occurs at the bottom of the gel.

band in the transfected membranes comigrated with the native ryanodine receptor of sarcoplasmic reticulum, the two bands being superimposed when these membranes were mixed and separated in the same lane (Figure 2). These data indicate that COS-1 cells transfected with plasmid pSRRI are capable of synthesizing a protein indistinguishable in immunoreactivity and molecular size from the native ryanodine receptor of skeletal muscle. In addition to the major polypeptide, minor bands of lower molecular weight were detected in transfected cells but not in control cells. These minor bands were assumed to be degradation products of the expressed protein since the ryanodine receptor is known to be highly susceptible to proteolytic degradation (Seiler et al., 1984; Imagawa et al., 1987). To minimize degradation, COS-1 cell microsomes were always prepared at 4 °C in the presence of various protease inhibitors. Omission of the protease inhibitors during membrane preparation resulted in greatly increased levels of the lower molecular weight bands and the disappearance of the high molecular weight band (data not shown).

Immunocytochemical Staining of Transfected and Control COS-1 Cells. Previous studies have shown that sarcoplasmic reticulum proteins expressed in COS-1 cells are consistently localized in the intracellular organelle membranes of the transfected cells (Maruyama & MacLennan, 1988; Leberer et al., 1989; Fujii et al., 1989). To study the distribution of the expressed ryanodine receptor in COS-1 cells and to monitor the transfection efficiency, immunocytochemical staining of whole cells was applied. Figure 3 shows the immunocytochemical staining of COS-1 cells transfected with pSRRI or fast-twitch Ca^{2+}-ATPase cDNA using monoclonal antibodies 34C or A52 (Maruyama & MacLennan, 1988). Staining was found only in COS-1 cells transfected with either pSRRI or Ca^{2+}-ATPase cDNA and not in control cells, confirming the specific expression of the ryanodine receptor, as shown by immunoblotting. An average of about 1–2% of cells were transfected with pSRRI and 5–10% of cells with Ca^{2+}-ATPase cDNA. Similar cellular staining patterns were observed in COS-1 cells transfected with pSRRI or Ca^{2+}-

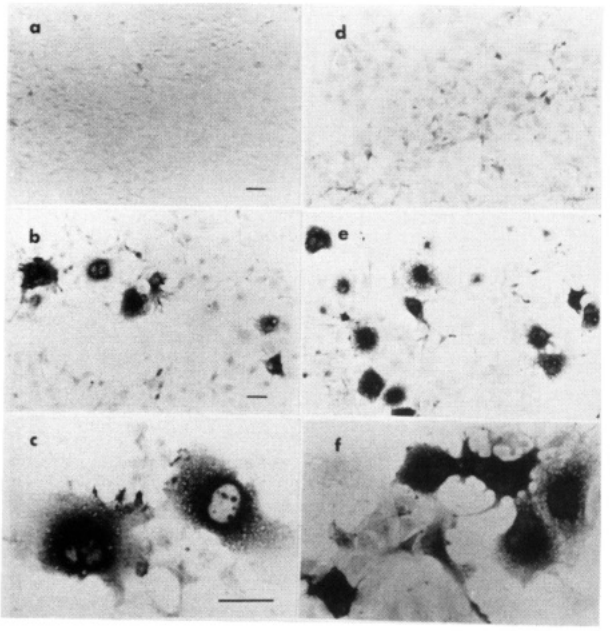

FIGURE 3: Immunocytochemical staining of ryanodine receptors and Ca^{2+}-ATPases expressed in COS-1 cells. COS-1 cells were transfected with pSRRI (b, c) or Ca^{2+}-ATPase cDNA (e, f) or no DNA (a, d). Cells were fixed and permeabilized 40–48 h after transfection. Expressed ryanodine receptors and Ca^{2+}-ATPases were detected by immunochemical staining using monoclonal antibodies 34C and A52, respectively, and secondary horseradish peroxidase-conjugated anti-mouse IgG. Bars = 50 μm.

ATPase cDNA, suggesting that the expressed ryanodine receptor and Ca^{2+}-ATPase have similar intracellular distributions within COS-1 cells, as expected.

[^{3}H]Ryanodine Binding to Membrane Preparations from Transfected and Control COS-1 Cells. In order to establish whether the expressed protein formed a ryanodine binding site, we carried out a radioligand binding assay using [^{3}H]-ryanodine. Figure 4 shows that membrane preparations from transfected COS-1 cells exhibited a saturable and specific binding of [^{3}H]ryanodine, whereas no significant [^{3}H]-ryanodine binding was observed in similar preparations from control cells. The Scatchard analysis shown in Figure 4a yielded a B_{max} of 0.22 ± 0.07 pmol/mg of protein and a K_d of 16.2 ± 1.16 nM (mean ± SE, n = 3). This binding affinity is similar to the K_d of 19 nM reported by Takeshima et al. (1989) for the ryanodine receptor expressed in CHO cells and also to that observed in purified preparations of native receptor (Imagawa et al., 1987; Lai et al., 1988). Binding parameters for the native ryanodine receptor of rabbit skeletal muscle heavy sarcoplasmic reticulum are shown in Figure 4b. In our hands, the B_{max} was 7.9 ± 1.04 pmol/mg of protein, and the K_d was 7.6 ± 1.15 nM (mean ± SE, n = 3, Figure 4b). Thus, the expressed protein is capable of binding [^{3}H]ryanodine with a similar binding affinity to that observed in the native sarcoplasmic reticulum. Since ryanodine binds with high affinity to a tetrameric form of the protein (Lai et al., 1989; Anderson et al., 1989), these data suggest that the ryanodine receptor expressed transiently in COS-1 cells may also form a tetrameric complex. If this is the case, the level of tetrameric ryanodine receptor expressed in COS-1 cells can be calculated on the basis of high-affinity ryanodine binding sites. Assuming there is one ryanodine binding site per assembled tetramer, a pure ryanodine receptor complex of mass 2 400 000 daltons should bind about 400 pmol of ryanodine/mg of protein (Imagawa et al., 1987; Lai et al., 1988). Thus, our protein in the COS-1 microsomal fraction is about 0.05% pure (0.22/400 pmol/mg) and about 30–40-fold (7.9/0.22 pmol/mg)

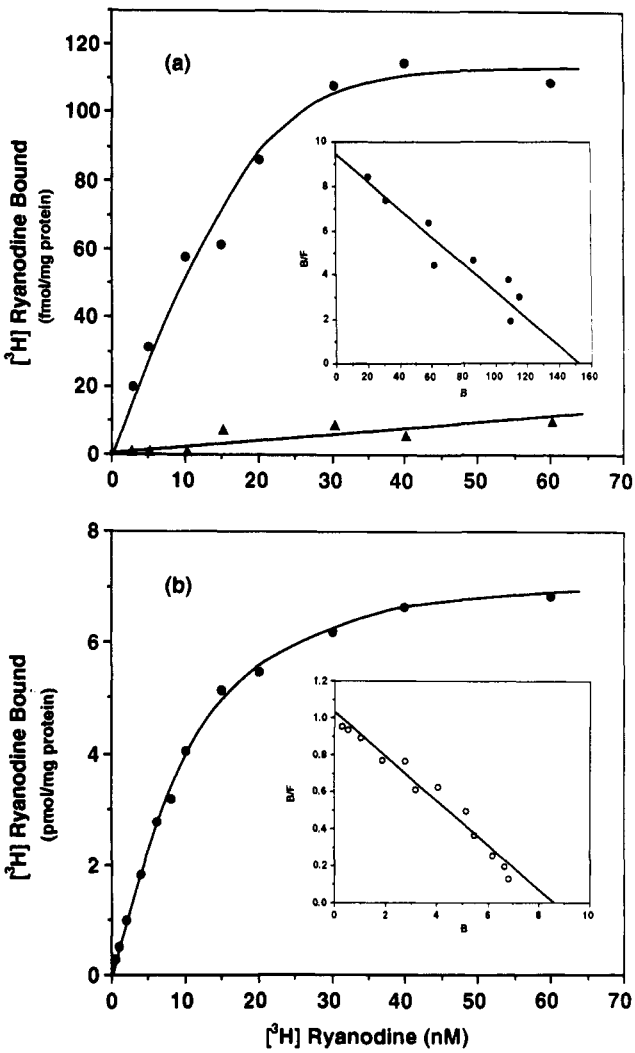

FIGURE 4: [^{3}H]Ryanodine binding to membrane preparations of transfected and control cells and to sarcoplasmic reticulum. Membrane proteins (0.5–1 mg/mL) were incubated with various concentrations (1–60 nM) of [^{3}H]ryanodine at 37 °C for 1 h. [^{3}H]Ryanodine binding was determined by membrane filtration as described under Experimental Procedures. (a) [^{3}H]Ryanodine binding to membrane preparations from transfected (circles) or control (triangles) COS-1 cells. (b) [^{3}H]ryanodine binding to sarcoplasmic reticulum. Scatchard analyses (insets) yielded an apparent B_{max} of 0.22 ± 0.07 pmol/mg and a K_d of 16.2 ± 1.16 nM (mean ± SE, n = 3) for ryanodine binding to the expressed ryanodine receptor and a B_{max} of 7.9 ± 1.04 pmol/mg and K_d of 7.6 ± 1.15 nM (mean ± SE, n = 3) for ryanodine binding to the sarcoplasmic reticulum. Data shown are from representative experiments done in duplicate.

more dilute than a purified preparation of ryanodine receptor from junctional sarcoplasmic reticulum.

As further confirmation that the expressed ryanodine receptor, like the native receptor, assembled as a large oligomeric complex, CHAPS-solubilized membranes from transfected and control COS-1 cells and from native junctional sarcoplasmic reticulum were subjected to sucrose density gradient centrifugation (Lai et al., 1988). Figure 5 shows the distribution of the expressed ryanodine receptor in a linear sucrose density gradient as determined by an enzyme-linked immunoabsorbent assay using mAb 34C. Immunoreactivity was found in the bottom half of the gradient of the solubilized membrane preparation from transfected COS-1 cells. The sedimentation of immunoreactivity from the transfected membrane preparation was identical to that of solubilized native receptors. On the other hand, no significant immunoreactivity was detected in gradients of solubilized control COS-1 cells. These results suggest that the expressed protein,

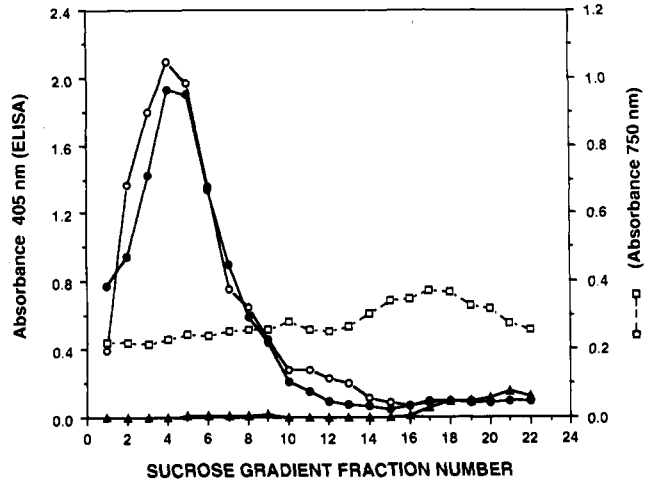

FIGURE 5: Enzyme-linked immunoabsorbent assay of sucrose density gradient fractions of solubilized membrane preparations from transfected and control COS-1 cells and sarcoplasmic reticulum. Membrane preparations from transfected (filled circles) or control (triangles) COS-1 cells (5 mg) or (open circles) sarcoplasmic reticulum (0.5 mg) were solubilized with CHAPS and fractionated by 10–30% (w/v) linear sucrose density gradient centrifugation. Gradient fractions (0.5 mL/fraction) were collected from the bottoms of the tubes. The absorbance at 750 nm (squares) was monitored according to Lowry et al. (1951). Only the absorbance for the transfected membrane preparation is shown. Aliquots of gradient fractions from transfected or control membrane preparations (50 μL) or sarcoplasmic reticulum (10 μL) were used for the enzyme-linked immunoabsorbent assay (ELISA). Fraction 1 was eluted from the bottom of the gradient.

indeed, formed a large oligomeric complex, similar to that formed by the native receptor. The total amount of immunoreactivity determined by the enzyme-linked immunoabsorbent assay was similar to that of solubilized sarcoplasmic reticulum, in spite of the fact that 50 times less sarcoplasmic reticulum protein was used (Figure 5). These results confirm that the amount of expressed ryanodine receptors in COS-1 cells is about 50 times less than that found in sarcoplasmic reticulum and are consistent with the expression levels estimated from the [^{3}H]ryanodine binding assay (Figure 4).

Single-Channel Recordings of the Expressed Ryanodine Receptor. The ionophoric properties of the expressed ryanodine receptor were established using single-channel recordings in planar bilayers. In these experiments, the expressed ryanodine receptor was purified as in Figure 5, concentrated using Centricon-100 microconcentrators, and added to the cis solution as described by Smith et al. (1988). Extensive controls showed that Ca^{2+} release channel activity was not present in sucrose gradient fractions prepared in the same manner from nontransfected cells (data not shown). Figure 6 shows a recording of expressed ryanodine receptors, solubilized and concentrated as described above. The data correspond to about 21 s of uninterrupted activity, divided into 24 traces. Recordings of large numbers of opening and closing events from 1 or more channels of the type shown in Figure 6 were made on at least 13 separate occasions with an average recording time of 12 min per bilayer and a total compiled recording time from these 13 bilayers of 158 min. The activity of the expressed receptors was characterized by the presence of multiple conductance states and at least one fast and one slow gating mode. Traces 3–10 of Figure 6 correspond to a segment in which the slow gating mode, composed of long-duration open and closed events, was preferentially observed. Traces 12–17 depict the fast gating mode, in which the conductance is comparatively higher and there is fast flickering between open and closed states. The end of the fast gating mode and the reappearance of the slow

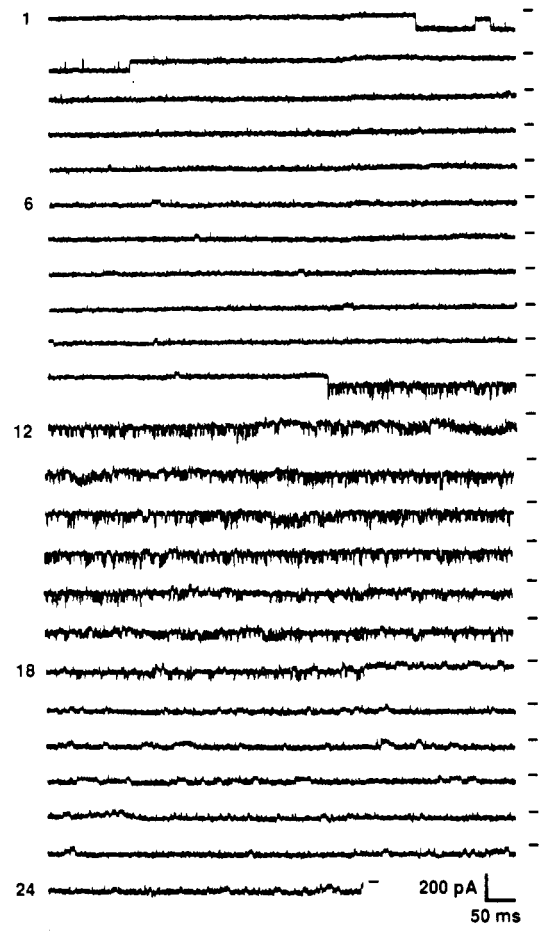

FIGURE 6: Single-channel recording of the expressed ryanodine receptor. Uninterrupted activity during 21 s is shown. Traces are labeled 1–24. The holding potential was –60 mV. Base-line current is indicated to the right of each trace.

gating mode at trace 18 strongly suggest that the fast and slow gating behaviors represent a kinetic switch within the same expressed receptor rather than overlapping activities of two independent, kinetically-different channels.

Fast and slow gating modes were observed in numerous recordings, so we compared their kinetics to those of native Ca^{2+} release channels under the same conditions. Native channels were incorporated into planar bilayers by fusion of rabbit skeletal muscle heavy sarcoplasmic reticulum as described elsewhere (Coronado et al., 1992). Left (A, D, G) and center (B, E, H) panels of Figure 7 describe the properties of the slow and fast gating modes of the expressed channel, respectively, whereas the right (C, F, I) panel corresponds to the same analysis in the native channel. Two conductance states of 640 and 300 pS were identified in the native channel, as indicated by the arrows in Figure 7C and by the histograms of current amplitude (Figure 7F). A histogram of open channel duration for the 640-pS state in Figure 7I revealed a single lifetime of 0.8 ms. Both the Cs^+ conductance and the channel lifetime agreed well with previous reports by Smith et al. (1988) and Kawano and Coronado (1992). We also identified two conductance states in the fast gating mode of the expressed channel (see arrows in Figure 7B), but the mean values are larger than those of the native channel (800 and 490 pS). Although the mean conductances of the fast gating mode of the expressed channel and those of the native channel were different, a significant proportion of events occurring during the fast gating mode had conductances similar to those of native channels. For example, in the 490-pS histogram of Figure 7E, 10% of events were less than 330 pS, and 8% were more than 600 pS. The gating kinetics of the fast mode agreed well with those of native channels, as indicated by the fact that the histogram of durations of the 800-pS state (Figure 7H) was best fit by time constants of 0.4 and 1.6 ms. These values are within a factor of 2 of the single lifetime of the native Ca^{2+} release channel. In contrast to the fast mode, the unit conductance of the slow gating mode (Figure 7D) was similar to the large conductance state of the native channel (620 vs 640 pS), yet the kinetics were markedly different. The slow gating mode of the expressed channel (Figure 7G) was characterized by long-term openings reminiscent of Ca^{2+} release channels activated by adenine nucleotides (Smith et al., 1985).

Native Ca^{2+} release channels are activated by cytosolic ligands such as adenine nucleotides and Ca^{2+} and are blocked by Mg^{2+} and ruthenium red (Smith et al., 1985, 1986, 1988). We therefore determined whether a similar ligand dependence was present in the expressed protein. Because the open probability was variable, being high during the slow gating mode but considerably lower in the fast gating mode, a quiescent control channel was chosen so that the stimulatory effects of Ca^{2+} and ATP would be immediately obvious. Figure 8 shows an experiment in which the sequence of additions to the cis chamber following the control period was as follows: (1) 5 mM ATP, (2) 100 μM $CaCl_2$, (3) 10 mM $MgCl_2$, and (4) 10 μM ruthenium red. Control activity was monitored during 90 s at –20 mV, followed by 90 s at voltages in the range of –30 to –50 mV and a final 15-s period at –20 mV before addition of ligands. Open probability was calculated for each section of the experiment (control through 4) by monitoring the duration of events at –20 mV during the times indicated in parentheses. During the two –20-mV sections of the control (105-s total), we observed a single 7-ms opening which appears as a brief spike in Figure 8. Thus, the open probability during the control period was essentially zero. As is clear from the recordings, the two stimulatory ligands produced a dramatic increase in channel activity. Open probability increased to 0.05 after addition of ATP (150 s) and to 0.5 after addition of Ca^{2+} (60 s). Subsequently, Mg^{2+} (34 s) partially blocked the activated channel, while ruthenium red (57 s) caused irreversible blockage of all openings, but only after a brief period at +20 mV. The total number of events captured after each ligand addition was 1 during control, 135 after ATP, 50 after Ca^{2+}, 3 after Mg^{2+}, and none after ruthenium red. On the basis of the time used to calculate open probability, the event presentation rate was 0.01, 0.9, 1.2, and 0.09 event/s for control, ATP, Ca^{2+}, and Mg^{2+}, respectively.

In this experiment, openings during activation by ATP were to a rather large conductance state of 5.5 nS. In the presence of both Ca^{2+} and ATP, two conductance states of 4.4 and 3.1 nS were observed. Since all of the conductances were activated by the stimulatory ligands and fully blocked by ruthenium red, they almost certainly originated from the ryanodine receptor expressed in COS-1 cells. On the basis of these results, we concluded that the expressed receptor was gated in a manner consistent with native Ca^{2+} release channels. However, results tended to be variable, especially with respect to the inhibitory ligands. Out of seven experiments, 2/2 demonstrated activation by Ca^{2+}, 1/1 activation by ATP, 1/2 inhibition by Mg^{2+}, and 1/3 inhibition by ruthenium red.

The interaction of the native Ca^{2+} release channel with ryanodine results in a slowing of channel kinetics and a characteristic decrease in conductance (Lai et al., 1988; Smith et al., 1988). Since these changes are specific for Ca^{2+} release channels, it was important to establish whether this transformation occurred in the expressed protein. The changes in

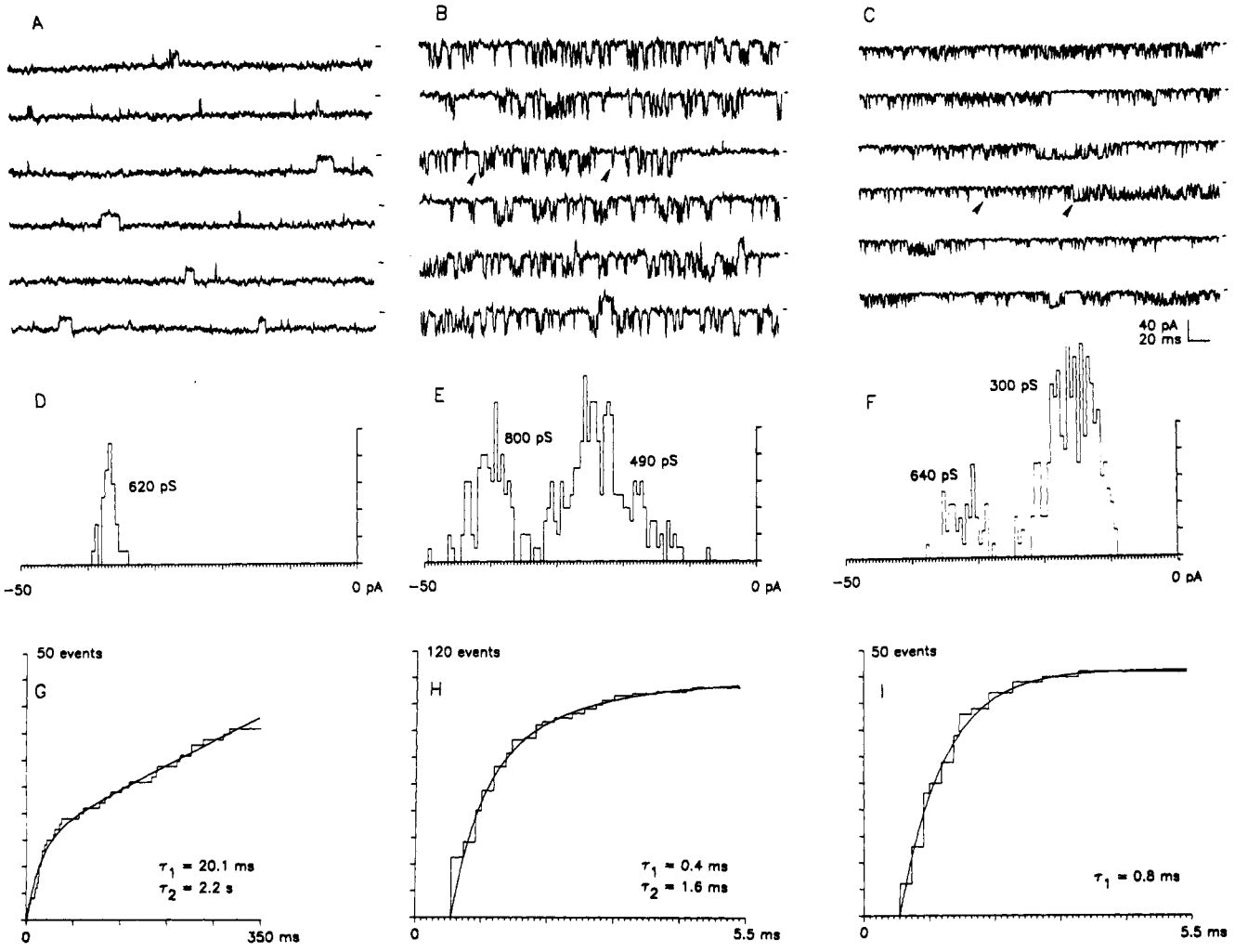

FIGURE 7: Comparison of the kinetic and conductive properties of expressed and native Ca^{2+} release channels. All recordings were made in symmetrical 380 mM CsCl-containing solutions as described under Experimental Procedures. Panels A, D, and G correspond to selected single-channel records, a current amplitude histogram, and a cumulative histogram of channel durations for the slow-gating mode of the expressed channel, respectively. Panels B, E, and H correspond to the same analyses of the fast-gating mode of the expressed channel. Panels C, F, and I correspond to the same analyses of a native Ca^{2+} release channel of rabbit skeletal muscle. Single-channel recordings were made at −60 mV (A) or −50 mV (B, C). Arrows in the single-channel recordings indicate representative conductance states identified in the current amplitude histograms. The *y*-axes in the current amplitude histograms D, E, and F correspond to 2 events/division. Histograms of durations (G, H, I) were fit by the sum of one or two exponentials with the time constants indicated in each graph.

the conductive properties of the expressed channel induced by ryanodine are shown in Figure 9. The control period shown in the top panel corresponds to 4 s out of a total of 200 s during which only the fast gating type of kinetics was observed, with the exception of 2 s of a slow gating mode. The most frequent conductance during the control period was 1.1 nS, corresponding to that shown in the top panel of Figure 9. Following addition of 4 μM ryanodine to the cis chamber, the fast gating continued unaltered during 140 s. This was followed by an abrupt and essentially irreversible change in conductance, as shown in the bottom panel of Figure 9. The mean conductance of the ryanodine-modified channel was 410 pS, which corresponded to a fractional decrease in conductance of 63% relative to control. The channel remained at that conductance level for the next 104 s, except for approximately 2 s during which the channel returned to a high conductance with fast gating. The records also showed that this ryanodine-modified channel exhibited a greater proportion of longer openings relative to control, thereby leading to an overall increase in open probability from 0.79 in control to 0.98 after modification by ryanodine. A similar result demonstrating the effect of ryanodine on the expressed channel was obtained in one other experiment, but in this case, the percent decrease in the conductance was 77% (data not shown). In identical solutions to those used in Figure 9, the conductance of the native Ca^{2+} release channel was decreased by 58% following the addition of 10 μM ryanodine (data not shown). The latency of the kinetic transformation, the fractional decrease in conductance, and the increase in open duration are hallmarks of the transformation of a native channel by ryanodine and, therefore, confirm that ryanodine interacts with the expressed channel in a manner similar to that reported in native sarcoplasmic reticulum (Imagawa et al., 1987).

DISCUSSION

Skeletal muscle ryanodine receptors have been expressed in CHO cells and shown to increase the Ca^{2+} permeability of intracellular stores when exposed to caffeine or ryanodine (Penner et al., 1989). Although such results showed that the skeletal muscle ryanodine receptor can assemble into a pharmacologically competent channel when expressed in a nonmuscle cell, no evidence was presented of modulation of the expressed channel by Ca^{2+}, ATP, or Mg^{2+}, the physiological ligands which control gating in striated muscle. Indirect evidence for the presence of Ca^{2+} and ATP binding sites within the ryanodine receptor was previously based on sequence homology to other Ca^{2+} and nucleotide binding proteins (Takeshima et al., 1989; Zorzato et al., 1990).

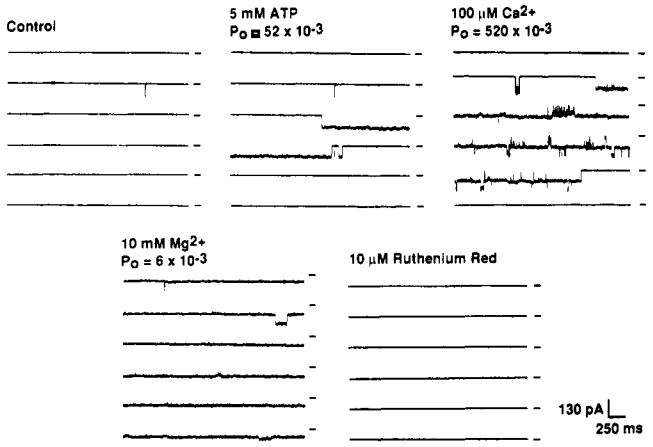

FIGURE 8: Effect of ATP, Ca^{2+}, Mg^{2+}, and ruthenium red on the open probability (P_o) of a ryanodine receptor expressed in COS-1 cells. All traces are from the same bilayer and were selected to indicate the average activity in each condition. Open probability (P_o) was measured separately following each change in ligand concentration. One opening was seen during the control period, and no openings were seen during the ruthenium red period. A leak current developed near the end of the recording period in Ca^{2+} and lasted throughout the period in Mg^{2+} and the beginning of the period in ruthenium red. This leak current was subtracted prior to calculation of the P_o for the Mg^{2+} period. All recordings were made at −20 mV. Base-line current is indicated to the right of each trace.

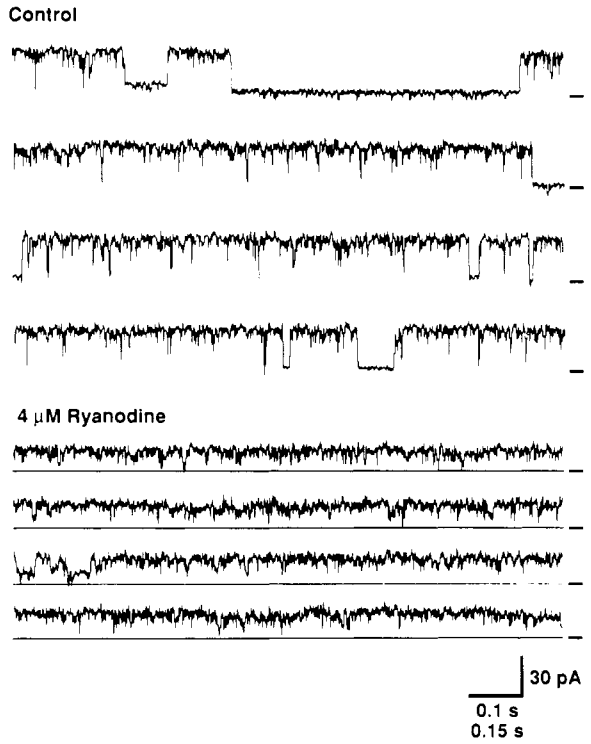

FIGURE 9: Effect of ryanodine on the COS-1 cell-expressed ryanodine receptor. Displayed recordings were made at +25 mV and are from the same bilayer. The time calibration bar represents 0.1 s for the top control panel and 0.15 s for the bottom panel. Base-line current is indicated to the right of each trace.

In the present study, we expressed the skeletal muscle ryanodine receptor cDNA in COS-1 cells and purified the protein complex in order to identify the single-channel characteristics and the ligand-dependent gating properties of the expressed protein. The following results establish that the expressed protein was similar to ryanodine receptors from native sarcoplasmic reticulum: (1) The expressed ryanodine receptor was indistinguishable from the native ryanodine receptor in molecular size and immunoreactivity (Figure 2); (2) Scatchard analysis of ryanodine binding yielded a B_{max} of 0.22 pmol/mg of protein and a K_d of 16.2 nM for the transfected membrane preparation, and a B_{max} of 7.9 pmol/mg of protein and K_d of 7.6 nM for isolated junctional sarcoplasmic reticulum, indicating that the expressed ryanodine receptor formed a functional ryanodine binding site (Figure 4); (3) cosedimentation of the expressed and native ryanodine receptors in a linear sucrose density gradient established that the expressed ryanodine receptor formed an oligomeric complex similar to that formed by the native receptor (Figure 5); (4) when incorporated into planar lipid bilayers, the expressed ryanodine receptor formed a channel with gating modified by Ca^{2+}, ATP, Mg^{2+}, ruthenium red, and ryanodine (Figures 8 and 9). Our experiments show that the ryanodine receptor cDNA encodes all of those binding sites presently believed to be relevant to the control of gating of the native Ca^{2+} release channel. As a corollary, they provide no support for the postulate that the 106-kDa protein (Zaidi et al., 1989) is an essential component of a functional Ca^{2+} release channel.

In contrast to the structural and functional similarities described above, there were noticeable similarities and differences in the kinetic and conductive features of the expressed and native channels. In addition to a fast gating mode analogous to that of the native channel, the expressed channel exhibited a slow gating mode seldom seen in native channels (Figure 7). The mean conductance of the slow mode (620 pS) agreed well with one of the two conductances of the native channel (640 pS). The fast gating mode exhibited the same kinetics as the native channel, but the conductance states were significantly higher.

Four conductance states up to 800 pS have been consistently reported for native channels (Ma et al., 1988; Smith et al., 1988; Liu et al., 1989), but the larger conductance states of the expressed channel (≥1 nS) have not been identified in native sarcoplasmic reticulum. The anomalous conductances of the expressed channel may represent an altered structure of the receptor, originating from one or more factors, such as the oligomeric state or the degree of proteolytic degradation of the expressed receptor. A structural alteration of a fraction of the expressed receptors could also be inferred from the numerous experiments in which Mg^{2+} or ruthenium red failed to close the channel. It is important to note, however, that there was no correlation between the conductance and the presence or absence of ligand dependence, as indicated by the experiment in Figure 8 where channels with unusually large conductances (≥1 nS) responded correctly to stimulatory and inhibitory ligands. Given the oligomeric nature of the pore, the higher conductance states of the expressed channel could reflect an oligomeric structure of the expressed receptor not present in native sarcoplasmic reticulum. This could be caused by differences in specific posttranslational modification of the ryanodine receptor between COS-1 and muscle cells. In principle, if oligomers larger than tetramers were formed, they could be identified by their mobility in sucrose density gradients (Lai et al., 1988). In practice, however, the difference in density between a tetramer, a pentamer, or a hexamer may not be large enough to permit a clear physical separation. Thus, purification techniques that yield functional channel activity, such as the sucrose gradient method, will have to be improved before this possibility can be addressed experimentally.

Usually large conductance states could also arise from proteolytic degradation of the receptor. Large, noisy conductances have been observed after extensive proteolytic cleavage of the sarcoplasmic reticulum incorporated into planar

lipid bilayers, although under limited proteolysis by trypsin the open probability, but not the conductance of the ryanodine receptor, appears to be increased (Meissner et al., 1989). We tested whether large conductances could originate from proteolyzed ryanodine receptors by attempting to record channels from a highly trypsinized preparation of native ryanodine receptor purified by sucrose density gradient centrifugation. In four out of four recordings, no unusually large conductances were observed (data not shown). Thus, proteolytic degradation of the expressed receptor during purification is an unlikely explanation for the observed differences in conductance.

It is also possible that a muscle-specific protein is required for the expression of ryanodine receptors with all the kinetic and gating properties described for the native channel. At least two sarcoplasmic reticulum proteins, triadin [a 95-kDa protein (Kim et al., 1990)] and FK506 binding protein [a 12-kDa polypeptide (Jayaraman et al., 1992)], are believed to interact with the ryanodine receptor. The modulatory action of these proteins on Ca^{2+} release channel function has not been characterized. Triadin has been postulated to form a physical and, possibly, a functional link between the dihydropyridine receptor and the ryanodine receptor. However, there is no evidence for the presence of triadin in those highly purified ryanodine receptors which have been shown to have native gating properties in previous studies (Smith et al., 1988). By contrast, the FK506 binding protein has been shown to be present in all standard preparations of purified ryanodine receptors in amounts that may be stoichiometric with the 564-kDa subunit.

The conductance of the receptor could also be modulated by the environment within a given tissue. For example, cardiac ryanodine receptors from different regions of the heart are known to differ in single-channel conductance (Borgatta et al., 1991). Interestingly, these differences disappear when the channels are assayed in a purified state (Xu et al., 1992), suggesting that there may be modulation of the conductance by components of the native membrane. Another example in a different channel is the tissue-specific β subunit of the dihydropyridine-sensitive L-type Ca^{2+} channel (Perez-Reyes et al., 1992). Coexpression in COS-1 cells of cardiac β and cardiac α_1 subunits, encoding the pore and drug binding components of the L-type Ca^{2+} channel, leads to the correction of kinetic and pharmacological anomalies seen when α_1 is expressed alone. A cardiac β subunit was not previously identified in purified complexes of cardiac dihydropyridine receptors (Hosey & Lazdunski, 1988), implying that a labile interaction of a channel and "unknown subunits" could have a large impact on channel function.

The optimization of transfection conditions for the expression of the ryanodine receptor cDNA has been a concern in this study. Since transfection efficiency is a limiting factor in COS-1 cell expression systems (Maruyama & MacLennan, 1988), the transfection efficiency was monitored by immunocytochemical staining. Despite intensive effort spent on optimization, only 1–2% of COS-1 cells were transfected by pSRRI using the DEAE-dextran method, whereas the transfection efficiency for Ca^{2+}-ATPase cDNA was found to be 5–10% using the same transfection conditions. Since cotransfection with both pSRRI and Ca^{2+}-ATPase cDNA had no significant effect on the transfection efficiencies of either of these cDNAs (data not shown), the difference in transfection efficiency may have been due to the large size of the ryanodine receptor cDNA rather than to its toxicity. The ryanodine receptor cDNA is 5 times as long as the ATPase cDNA and is possibly the largest cDNA yet expressed transiently. Alternative transfection methods such as electroporation or liposome-mediated transfection have been evaluated, but do not increase transfection efficiencies. Physical engulfment of such a large cDNA, in an expressible form, may be a limiting factor in transfection experiments, regardless of how they are performed. In support of this view, we have been able to express the NH_2-terminal 2600 bp of the ryanodine receptor at efficiencies comparable to those of the Ca^{2+}-ATPase cDNA of similar size (data not shown), suggesting that cDNA size is an important factor in transient transfection. Although the transfection efficiency for the ryanodine receptor is low, the expression level in each transfected cell is very high. On the basis of [^{3}H]ryanodine binding and enzyme-linked immunoabsorbent assays, membrane preparations from transfected cells contain about 40–50-fold fewer ryanodine receptors than a comparable preparation of sarcoplasmic reticulum. Thus, if 2% of the cells were transfected, the average expression level in each transfected cell could be as high as that in muscle. Functional expression of the ryanodine receptor is the first step toward studies of structure–function relationships of the ryanodine receptor by site-directed mutagenesis. Coexpression of ryanodine receptors and other sarcoplasmic reticulum proteins could then provide a system to study protein–protein interactions and the mechanism of excitation–contraction coupling.

ACKNOWLEDGMENT

We thank Dr. Francesco Zorzato for advice on recombinant DNA technology, Dr. Henry Krause for advice on immunocytochemical staining, Kazimierz Kurzydlowski for expert and invaluable technical assistance, Dr. John L. Sutko, University of Nevada School of Medicine, Reno, NV, for the gift of the monoclonal antibody 34C, Dr. Randal J. Kaufman, Genetics Institute, Boston, MA, for the gift of the expression vector pMT2(*Cla*I,*Xba*I), and Dr. Seiko Kawano for assistance in the initial single-channel recordings.

REFERENCES

Airey, J. A., Beck, C. F., Murakami, K., Tanksley, S. J., Deerinck, T. J., Ellisman, M. H., & Sutko, J. L. (1990) *J. Biol. Chem. 265*, 14187–14194.

Anderson, K., Lai, F. A., Liu, Q.-Y., Rousseau, E., Erickson, H. P., & Meissner, G. (1989) *J. Biol. Chem. 264*, 1329–1335.

Block, B. A., Imagawa, T., Campbell, K. P., & Franzini-Armstrong, C. (1988) *J. Cell Biol. 107*, 2587–2600.

Borgatta, L., Watras, J., Katz, A. M., & Ehrlich, B. E. (1991) *Proc. Natl. Acad. Sci. U.S.A. 88*, 2486–2489.

Campbell, K. P., & MacLennan, D. H. (1981) *J. Biol. Chem. 256*, 4626–4632.

Chen, S. R. W., Vaughan, D., Coronado, R., & MacLennan, D. H. (1992) *Biophys. J. 61*, A22.

Coronado, R., Kawano, S., Lee, C. J., Valdivia, C., & Valdivia, H. H. (1992) *Methods Enzymol. 207*, 699–707.

Endo, M. (1985) *Curr. Top. Membr. Transp. 25*, 181–230.

Fujii, J., Maruyama, K., Tada, M., & MacLennan, D. H. (1989) *J. Biol. Chem. 264*, 12950–12955.

Gorman, C. (1985) in *DNA cloning: A Practical Approach* (Glover, D. M., Ed.) Vol. 2, pp 143–190, IRL Press, Washington, D.C.

Hosey, M., & Lazdunski, M. (1988) *J. Membr. Biol. 104*, 81.

Hymel, L., Inui, M., Fleischer, S., & Schindler, H. G. (1988) *Proc. Natl. Acad. Sci. U.S.A. 85*, 441–445.

Imagawa, T., Smith, J. S., Coronado, R., & Campbell, K. P. (1987) *J. Biol. Chem. 262*, 16636–16643.

Inui, M., Saito, A., & Fleischer, S. (1987) *J. Biol. Chem. 262*, 15637–15642.

Jayaraman, T., Brillantes, A. M., Timerman, A. P., Fleischer, S., Erdjument-Bromage, H., Tempst, P., & Marks, A. R. (1992) *J. Biol. Chem. 267*, 9474–9477.

Kaufman, R. J., Davies, M. V., Pathak, V. K., & Hershey, J. W. B. (1989) *Mol. Cell. Biol. 9*, 946–958.

Kawano, S., & Coronado, C. (1991) *Biophys. J. 59*, 600a.

Kim, K. C., Caswell, A. H., Talvenheimo, J. A., & Brandt, N. R. (1990) *Biochemsitry 29*, 9281–9289.

Laemmli, U. K. (1970) *Nature 227*, 680–685.

Lai, F. A., Erickson, H. P., Rousseau, E., Liu, Q. Y., & Meissner, G. (1988) *Nature 331*, 315–319.

Lai, F. A., Misra, M., Xu, L., Smith, H. A., & Meissner, G. (1989) *J. Biol. Chem. 264*, 16776–16785.

Leberer, E., Charuk, J. H. M., Clarke, D. M., Green, N. M., Zubrzycka-Gaam, E., & MacLennan, D. M. (1989) *J. Biol. Chem. 264*, 3484–3493.

Liu, Q. Y., Lai, A., Rousseau, E., Jones, R. V., & Meissner, G. (1989) *Biophys. J. 55*, 415–424.

Lowry, O. H., Rosebrough, N. J., Farr, A. L., & Randall, R. J. (1951) *J. Biol. Chem. 193*, 265–275.

Ma, J., Fill, M., Knudson, C. M., Imagawa, T., Campbell, K. P., & Coronado, R. (1988) *Science 242*, 99–102.

Maruyama, K., & MacLennan, D. H. (1988) *Proc. Natl. Acad. Sci. U.S.A. 85*, 3314–3318.

Meissner, G., Rousseau, E., & Lai, F. A. (1989) *J. Biol. Chem. 264*, 1715–1722.

Penner, R., Neher, E., Takeshima, H., Nishimura, S., & Numa, S. (1989) *FEBS Lett. 259*, 217–221.

Perez-Reyes, E., Castellano, A., Kim, H. S., Bertrand, P., Baggstrom, E., Lacerda, A. E., Wei, X., & Bimbaumer, L. (1992) *J. Biol. Chem. 267*, 1792–1797.

Rardon, D. P., Cefali, D. C., Mitchell, R. D., Seiler, S. M., & Jones, L. R. (1989) *Circ. Res. 64*, 779–789.

Rios, E., & Pizarro, G. (1991) *Physiol. Rev. 71*, 849–908.

Saito, A., Inui, M., Radermacker, M., Frank, J., & Fleischer, S. (1988) *J. Cell Biol. 107*, 211–219.

Sambrook, J., Fritsch, E. F., & Maniatis, T. (1989) *Molecular Cloning, A Laboratory Manual*, Cold Spring Harbor Laboratory, Cold Spring Harbor, NY.

Seiler, S., Wegener, A. D., Whang, D. D., Hathway, D. R., & Jones, L. R. (1984) *J. Biol. Chem. 259*, 8550–8557.

Smith, J. S., Coronado, R., & Meissner, G. (1985) *Nature 316*, 446–449.

Smith, J. S., Coronado, R., & Meissner, G. (1986) *J. Gen. Physiol. 88*, 573–588.

Smith, J. S., Imagawa, T., Ma, J., Fill, M., Campbell, K. P., & Coronado, R. (1988) *J. Gen. Physiol. 92*, 1–26.

Takeshima, H. J., Nishimura, S., Matsumoto, T., Ishida, H., & Kangawa, K., Minamino, N., Matsuo, H., Ueda, M., Hanaoka, M., Hirose, T., & Numa, S. (1989) *Nature 339*, 439–445.

Towbin, H., Staehelin, T., & Gordon, J. (1979) *Proc. Natl. Acad. Sci. U.S.A. 76*, 4350–4354.

Vaughan, D. M., Chen, S. R. W., MacLennan, D. H., & Coronado, R. (1992) *Biophys. J. 61*, A130.

Wagenknecht, T., Grassucci, R., Frank, J., Saito, A., Inui, M., & Fleischer, S. (1989) *Nature 338*, 167–170.

Xu, L., El-Hashem, A., & Meissner, G. (1992) *Biophys. J. 61*, A245.

Zaidi, N. F., Lagenaur, C. F., Hilkert, R. J., Xiong, H., Abramson, J. J., & Salama, G. (1989) *J. Biol. Chem. 264*, 21737–21747.

Zorzato, F., Fujii, J., Otsu, K., Phillips, M., Green, N. M., Lai, F. A., Meissner, G., & MacLennan, D. H. (1990) *J. Biol. Chem. 265*, 2244–2256.